

SUPERVISED CONVOLUTIONAL NETWORKS FOR VOLUMETRIC DATA ENRICHMENT FROM LIMITED SECTIONAL DATA WITH ADAPTIVE SUPER RESOLUTION

Mitsuaki Matsuo¹, Kai Fukami^{2,1}, Taichi Nakamura¹, Masaki Morimoto¹, & Koji Fukagata¹

¹ Department of Mechanical Engineering, Keio University

² Department of Mechanical and Aerospace Engineering, University of California, Los Angeles

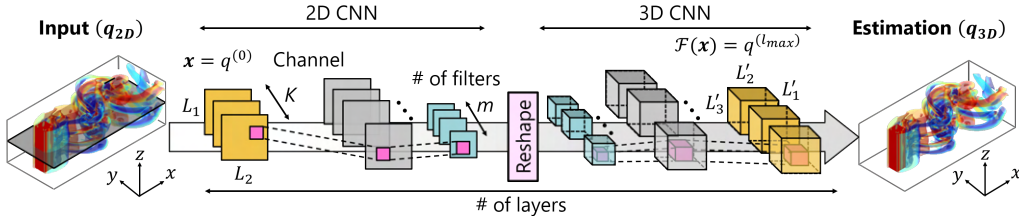


Figure 1: CNN-based volumetric data reconstruction from two-dimensional information.

ABSTRACT

We have recently encountered the tremendous improvement in computational power, which in turn causes insufficient utilization of big numerical data in a wide range of science and engineering due to storage and data-transfer limitations. Hence, of particular interest here is how we can handle big data, which are governed by strong chaoticity and nonlinearities, in an efficient manner. We here consider a supervised use of convolutional neural networks (CNNs) to achieve efficient data handling. The present CNN reconstructs three-dimensional (volumetric) data from limited two-dimensional information. As an example, a fluid flow around a square cylinder at $Re_D = 300$, which contains strong three-dimensional complexities, is considered. Our demonstration shows that the present framework can successfully estimate the three-dimensional flows from a few input sections, which eventually enables us to keep only sectional input data to obtain the whole information. We also propose a combination with an adaptive-sampling-based super-resolution analysis toward more effective data saving.

1 INTRODUCTION

The exponential growth in computing power is ongoing even today. This enables us to model a complex and nonlinear phenomenon with an immense number of spatio-temporal discretization. Computational fluid dynamics (CFD) is one of the understandable examples for this matter. It is widely known that the required number of spatial grid points for three-dimensional CFD is usually proportional to $Re^{9/4}$, where Re is the Reynolds number. In addition, the time scale ratio is proportional to $Re^{1/2}$, which implies the necessity of longer integration times with the precise time steps (Kajishima & Taira, 2017). Although this is just an example, we can now notice the importance to prepare an efficient way of data handling for a wide range of science and engineering, which enables us to achieve fast data transfer over the world and promotes the progress of science.

To that end, we here consider a three-dimensional data reconstruction from limited two-dimensional sectional measurements assisted by supervised convolutional neural networks. With an example of complex fluid flow around a square cylinder, we discuss the possibility of data compression and its effectiveness. In addition, we also propose an adaptive-sampling-based super resolution to achieve more efficient data saving.

2 METHODS

2.1 2D-3D CONVOLUTIONAL NEURAL NETWORK

We use convolutional neural network (CNN) (LeCun et al., 1998) for the present data reconstruction. Since our aim is to obtain a three-dimensional velocity field q_{3D} from two-dimension sectional

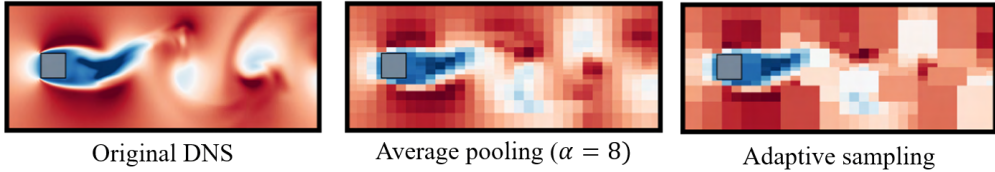


Figure 2: Comparison of different ways of spatial data sampling.

velocity fields \mathbf{q}_{2D} , we combine two- and three-dimensional CNNs, as illustrated in figure 1. The size of data will be explained later. As an activation function, we use ReLU function (Nair & Hinton, 2010) to stabilize the weight update process for training. Weights \mathbf{w} inside the present model \mathcal{F} are optimized in an L_2 error minimization manner as

$$\mathbf{w} = \operatorname{argmin}_{\mathbf{w}} \|\mathbf{q}_{3D} - \mathcal{F}(\mathbf{q}_{2D}; \mathbf{w})\|_2. \quad (1)$$

For the construction of the present model, we use early stopping criterion (Prechelt, 1998) with 20 iterations to avoid an overfitting (Brunton & Kutz, 2019).

2.2 ADAPTIVE SAMPLING BASED SUPER RESOLUTION

To deal with three-dimensional data in a more efficient manner, we also combine our three-dimensional reconstruction with super-resolution reconstruction (Fukami et al., 2019). We aim to reconstruct a three-dimensional field \mathbf{q}_{3D} from low-resolution sectional fields $\mathbf{q}_{2D,LR}$. Prior to the use of the aforementioned 2D-3D CNN, we prepare the another independent CNN \mathcal{G} for super resolution, such that $\mathbf{q}_{2D,HR} = \mathcal{G}(\mathbf{q}_{2D,LR}; \mathbf{w}_G)$. The whole pipeline is summarized as

$$\mathbf{q}_{3D} = \mathcal{F}(\mathbf{q}_{2D,HR}; \mathbf{w}) = \mathcal{F}(\mathcal{G}(\mathbf{q}_{2D,LR}; \mathbf{w}_G); \mathbf{w}). \quad (2)$$

Low-resolution data, utilized for training machine learning models in super resolution, is usually generated through max and average pooling operations (Fukami et al., 2019), as shown in the middle of figure 2. Though the pooling operations are simple and easy to apply, it may be inefficient to extract structures and features of data, especially when scales and complexities of structures significantly vary over the field. Hence, we here propose a new pooling idea referred to as *adaptive sampling* (see, Appendix for the detailed procedure) to consider a spatial ‘importance’ of local region for the determination of the sampling rate. A spatial standard deviation is used as the ‘importance’ of the local region, which reflects the larger significance of region as higher sampling ratio, as presented in the right side of figure 2. In the present demonstration, both the average-pooled field and the adaptive-sampled field are considered as an input $\mathbf{q}_{2D,LR}$ of the model for the super resolution \mathcal{G} and compared in terms of its efficacy.

3 RESULTS

As an example, a flow around a square cylinder at $Re_D = 300$ is considered. Since the wake at $Re_D = 300$ contains the complex three-dimensional structure caused by merging of separated shear layers (Bai & Alam, 2018), this setup can be regarded as a good demonstration to investigate whether the present CNN model works for complex data sets or not. The data set is prepared with a direct numerical simulation (DNS) by numerically solving the incompressible continuity and Navier–Stokes equations (Morimoto et al., 2020). In the present study, we focus on the part of computational volume around the square cylinder $(L_x, L_y, L_z) = (12.8D, 4D, 4D)$ with the grid number of $(N_x, N_y, N_z) = (256, 128, 160)$. We use 1000 snapshots for training the CNN model. As the input and the output attributes, the velocity fields $\mathbf{q} = \{u, v, w\}$ are used.

Let us first present the reconstructed flow field visualized with the λ_2 vortex criterion, i.e., $\lambda_2 = -0.001$ (Jeong & Hussian, 1995) in figure 3(a). We here use five and seven $x-y$ sectional velocities for the input data \mathbf{q}_{2D} . The reconstructed fields are in reasonable agreement with the reference DNS data. We also visualize the reconstructed sectional velocities at $z/D = 0.025$ in figure 3(b). As shown, the present model can reconstruct the flow field with reasonable accuracy in terms of both the visualization and the L_2 error norms. Notably, the reconstructed fields with $n_{\text{section}} = 7$ are almost indistinguishable from the reference, while capturing the fine structures. The results above supports the capability of the present model as an efficient data handling tool, which can reduce the data to approximately 4% ($= (256 \times 128 \times 7 \text{ sections}) / (256 \times 128 \times 160)$) of the original size.

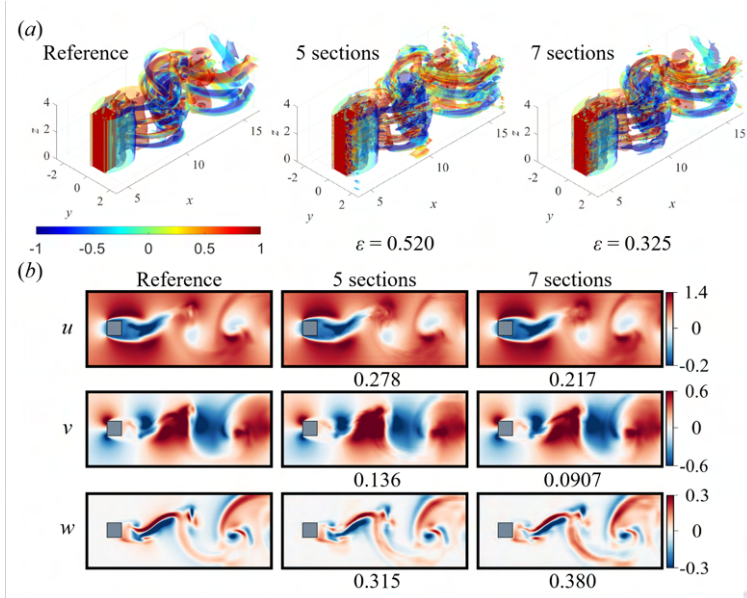


Figure 3: (a) CNN-based reconstruction fields with 5 and 7 cross sections (vortical structures identified with $\lambda_2 = -0.001$, colored by the streamwise vorticity). The values underneath each figure indicate an L_2 error norm. (b) Reconstructed sectional velocities at $z/D = 0.025$.

In addition to the aforementioned capabilities, the present model can be augmented combining with super-resolution analysis. As introduced in section 2.2, super-resolved velocity fields q_{HR} reconstructed from an adaptive-sampled low-resolution data q_{LR} are fed into the present 2D-3D CNN model \mathcal{F} as the input data. Prior to feed into the 2D-3D CNN model, the results on super-resolution analysis for two-dimensional sections are summarized in figure 4(a). For comparison, the results with conventional average pooling-based inputs are also presented. For the average pooling-based inputs, the high-resolution field of 256×128 grids can successfully be super-resolved from coarse input data of 16×16 grids. Moreover, the reconstruction accuracy can be improved with the adaptive sampling while also reducing the number of grid points on the low-resolution data. Especially, the number of grid points for the w component can be saved by approximately 25% against that with the average pooling. Note, however, that the adaptive sampling does not show the significant advantage for the u component in this particular example, although not shown in figure 4(a). This is due to the difference of complexity among velocity attributes, which implies that care should be taken for the choice of an appropriate pooling method depending on data sets. In turn, there may be an optimal combination of pooling methods to achieve efficient data handling.

We finally show the three-dimensional reconstructed fields from the super-resolved two-dimensional inputs in figure 4(b). We here use $n_{sections} = 5$ for all models. In addition to the uses of average pooling and adaptive sampling for all velocity attributes, the hybrid pooling, which uses the average pooling for the u component while taking the adaptive sampling for the v and w components, is also considered motivated by the observation above. The hybrid model can achieve almost same error label as that with the conventional average pooling while reducing the storage to approximately 0.0218% of the original number of grid points. Summarizing above, the present idea assisted by the supervised CNN framework with the adaptive super resolution can significantly reduce the data storage while keeping its reconstruction accuracy.

4 CONCLUDING REMARKS

We considered a supervised use of convolutional neural networks (CNNs) to reconstruct a three-dimensional flow field from limited sectional measurements toward effective data handling. The present report tested with a flow around a square cylinder at $Re_D = 300$ showed the capability of 2D-3D CNN for the reasonable reconstruction in terms of both the visualization assessments and the qualitative examinations, while saving the data storage of 0.02% assisted by the proposed adaptive

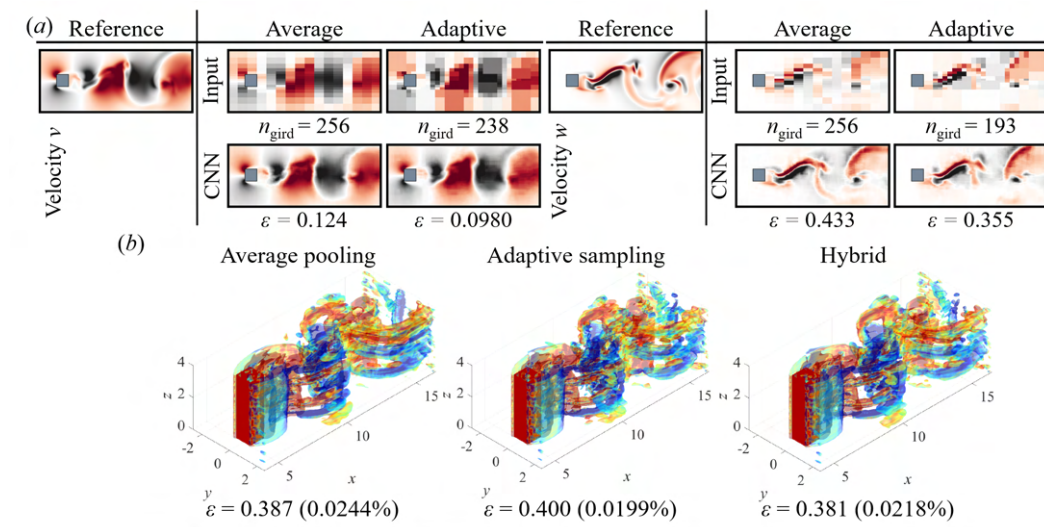


Figure 4: (a) Super-resolution reconstruction from adaptive sampled velocities v and w . The values underneath the contours of input indicate the number of grid points. The values below the contours indicate the L_2 error norm. (b) Reconstructed fields from coarse input combining the conventional pooling and the adaptive sampling. Listed values indicate the L_2 error and the compression ratio against the number of grid points over the original three-dimensional discretized domain.

sampling. The notable strength of the present model is its reversible manner for data compression, i.e., lossless compression, which should be appreciated not only in fluid mechanics but also in a wide range of science and engineering applications. The demonstration with the complex three-dimensional fluid flows here supports us to use the present idea for more practical applications such as chaotic turbulence and experimental data. For enthusiastic readers, we refer to Matsuo et al. (2021) in details.

REFERENCES

- H. Bai and M. M. Alam. Dependence of square cylinder wake on reynolds number. *Phys. Fluids*, 30:015102, 2018.
- S. L. Brunton and J. N. Kutz. *Data-Driven Science and Engineering: Machine Learning, Dynamical Systems, and control*. Cambridge University Press, 2019.
- K. Fukami, K. Fukagata, and K. Taira. Super-resolution reconstruction of turbulent flows with machine learning. *J. Fluid Mech.*, 870:106–120, 2019.
- J. Jeong and F. Hussian. On the identification of a vortex. *J. Fluid Mech.*, 285:69–94, 1995.
- T. Kajishima and K. Taira. *Computational Fluid Dynamics*. Springer International Publishing, 2017.
- Y. LeCun, L. Bottou, Y. Bengio, and P. Haffner. Gradient-based learning applied to document recognition. *Proc. IEEE*, 86(11):2278–2324, 1998.
- M. Matsuo, T. Nakamura, M. Morimoto, K. Fukami, and K. Fukagata. Supervised convolutional network for three-dimensional fluid data reconstruction from sectional flow fields with adaptive super-resolution assistance. arXiv:2103.09020, 2021.
- M. Morimoto, K. Fukami, and K. Fukagata. Experimental velocity data estimation for imperfect particle images using machine learning. arXiv:2005.00756, 2020.
- V. Nair and G. E. Hinton. Rectified linear units improve restricted boltzmann machines. *In Proc. 27th International Conference on Machine Learning*, 2010.
- L. Prechelt. Automatic early stopping using cross validation: quantifying the criteria. *Neural Netw.*, 11(4):761–767, 1998.

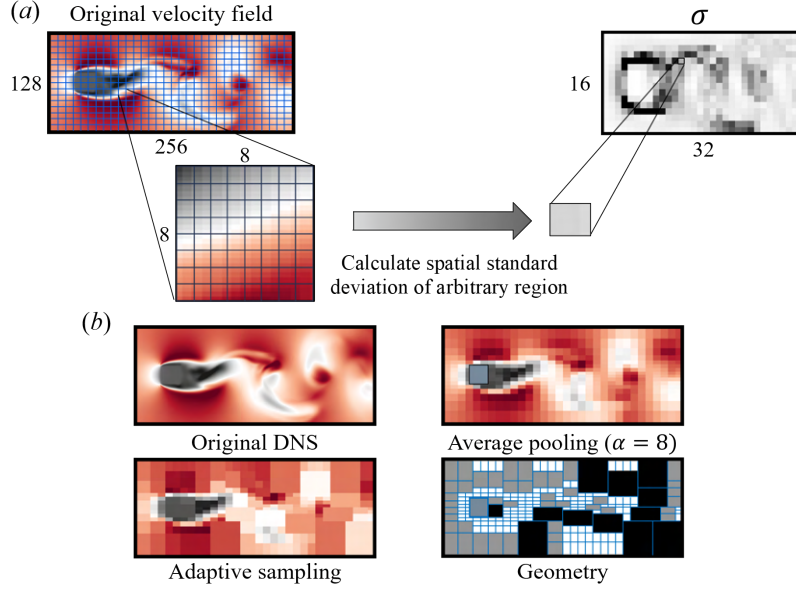


Figure 5: (a) A standard deviation map from velocity data with $N_{sw} \times N_{sh} = 8 \times 8$. (b) Application of the adaptive sampling to the present velocity field. For comparison, the standard average pooling with $\alpha = 8$ is also shown. The colors in the geometry image indicate the pooling rate α ; white represents $\alpha = 8$, gray represents 16 and black represents 32.

APPENDIX: ADAPTIVE SAMPLING

For the combination of the present three-dimensional reconstruction and super resolution, we use an adaptive-sampling-based input to achieve efficient data saving. In this Appendix, we explain the detailed procedure of adaptive sampling. A snapshot of velocity field is first divided into several sub-domains of $N_{sw} \times N_{sh}$, where N_{sw} and N_{sh} correspond to the width and the height of the sub-domain, respectively, as shown in figure 5(a). We then consider the local standard deviation based on the deviation from the mean in the sub-domain to decide the local pooling rate α for each snapshot. Throughout these processes, the standard deviation map $N_{\sigma,w} \times N_{\sigma,h}$ can be generated, where $N_{\sigma,w} = N_x/N_{sw}$, $N_{\sigma,h} = N_y/N_{sh}$, and $N_x \times N_y$ indicates the size of the entire cross-section. Based on the standard deviation map and the adaptive sampling rate α , the adaptive-sampling-based low-resolution data can be $N_{\sigma,w} \times N_{\sigma,h}$ arranged as follows:

1. Scan the standard deviation map and find the portion with smaller values than a certain threshold, i.e., $\sigma_{i,j} < \theta_{th,1}$.
2. Scan the portions surrounding $\sigma_{i,j}$, i.e., $\{\sigma_{i+1,j}, \sigma_{i+2,j}, \dots, \sigma_{i+(\alpha_1/N_{sw}-1),j+(\alpha_1/N_{sh}-1)}\}$. If all the portions have smaller standard deviations than $\theta_{th,1}$, we then take the pooling operation over $\sigma_{i,j}$ to $\sigma_{i+(\alpha_1/N_{sw}-1),j+(\alpha_1/N_{sh}-1)}$.
3. For remaining portion, scan over the standard deviation map again for an arbitrary portion with a standard deviation between the thresholds $\theta_{th,1} < \sigma_{ij} < \theta_{th,2}$.
4. Similarly, if the surrounding portion has thresholds less than $\theta_{th,2}$, we take the pooling operation over $\sigma_{i,j}$ to $\sigma_{i+(\alpha_2/N_{sw}-1),j+(\alpha_2/N_{sh}-1)}$.
5. Take the standard average pooling operation for the remaining portions, where the standard deviation is higher than $\theta_{th,2}$.

As an example, let us present the adaptive sampled flow field with the pooling rates $\{\alpha_1, \alpha_2, \alpha_3\} = \{32, 16, 8\}$ in figure 5(b). As can be seen, the region with the higher standard deviation retains higher resolution than that with lower standard deviation. Note that we have the variation in the domain size for the same pooling rate since we consider the non-uniform grid in the y direction. More details can be found in Matsuo et al. (2021).